PHYSICAL REVIEW B **88**, 201407(R) (2013)

Secondary-electron emission induced by *in vacuo* surface excitations near a polycrystalline Al surface

Wolfgang S. M. Werner,* Francesc Salvat-Pujol,† Alessandra Bellissimo, Rahila Khalid, and Werner Smekal‡
Institut für Angewandte Physik, Vienna University of Technology, Wiedner Hauptstraße 8-10/134, A-1040 Vienna, Austria

Mihály Novák
Institute for Nuclear Research, Hungarian Academy of Sciences (MTA ATOMKI), 18/c Bem tér, H-4026 Debrecen, Hungary

Alessandro Ruocco and Giovanni Stefani
Dipartimento di Scienze and Unità CNISM, Università Roma Tre, via della Vasca Navale 84, I-00146 Rome, Italy
(Received 6 September 2013; published 27 November 2013)

The double-differential spectrum of coincidences between backscattered electrons and secondary electrons (SEs) emitted from a polycrystalline Al surface bombarded with 100-eV electrons was measured. For energy losses of the scattered electron in between the work function of Al and the bulk plasmon energy, a sharp peak is observed in the SE spectra, corresponding to ejection of a single electron near the Fermi edge receiving the full energy loss and momentum of the primary electron. This process predominantly takes place when the primary electron suffers a surface energy loss in vacuum, and leads to SE ejection from the very surface. At energy losses just above the bulk plasmon energy, a sharp transition is observed, corresponding to a sudden increase in the depth of ejection. The latter is a direct consequence of the complementarity of surface and bulk plasmons, the so-called Begrenzungs effect.

DOI: 10.1103/PhysRevB.88.201407 PACS number(s): 68.49.Jk, 79.20.−m, 79.60.−i

When an energetic electron strikes a solid surface it may transfer part of its energy to the solid-state electrons. If the energy transfer exceeds the work function of the solid, an electron near the Fermi edge may escape over the surface barrier as a secondary electron (SE) or may in turn suffer energy losses, giving rise to the formation of a cascade of slow electrons.[1–4] The above phenomenon of electron-induced SE emission is highly relevant in a broad variety of applications but, due to a lack of spectral features in the cascade, SE emission is still far from being quantitatively understood.[5] While the different excitation channels can be easily discriminated with electron-energy-loss spectroscopy, the mechanism by which the deposited energy is dissipated away over the degrees of freedom of the solid is not easily resolvable by experiment. It is obvious that this requires the detection of correlated electron *pairs*, where one electron carries the signature of the involved excitation, while the other provides information on its decay.[6–14]

This Rapid Communication presents the double-differential secondary-electron electron-energy-loss coincidence spectrum (SE2ELCS) of Al bombarded with 100-eV primary electrons. In the coincidence data, events can be distinguished in which the primary electron experiences a surface energy loss in vacuum, leading to ejection of a solid-state electron from the very surface (less than half an angstrom below the surface) that reaches the detector without traversing the solid at all. The choice of Al as the material for these investigations is motivated by the fact that the electron-solid interaction is characterized by a sharp surface and bulk plasmon, making it possible to distinguish the single- and multiple-scattering regime in experimental data with the bare eye, considerably simplifying the identification of relevant scattering processes.

The present SE2ELCS measurements were carried out in a coincidence spectrometer, measuring arrival-time differences of electron pairs in a hemispherical mirror analyzer (HMA, measuring the scattered electron, subscript s), and a time-of-flight analyzer (TOF, measuring the ejected electron, subscript e). The electron polar incidence angle amounted to $\theta_i = 60^\circ$, and detection took place at $\theta_{\mathrm{TOF}} = 0^\circ$ in the TOF and $\theta_{\mathrm{HMA}} = 60^\circ$ in the HMA. While the coincidence measurements were carried out with a continuous electron beam,[15,16] TOF single spectra were measured with a pulsed beam. Details of the experimental procedure are given in Refs. 15 and 16.

Figure 1 compares the TOF singles spectrum with the coincidence spectrum corresponding to scattered electrons that have suffered an arbitrary energy loss between 0 and 35 eV. Faint shoulders in the coincidence TOF spectrum are indicated at SE energies of $\hbar\omega_b - \Phi$ and $\hbar\omega_s - \Phi$, corresponding to decay of a volume or surface plasmon and subsequent emission of a SE that escapes with the full energy.[3,11] Here $\hbar\omega_s = 10.5$ eV and $\hbar\omega_b = 15.0$ eV represent the surface and bulk plasmon energy, respectively, and $\Phi = 4.2$ eV is the work function of the surface. Although it is clear that the energy transfer from the scattered to the ejected electron occurs in the course of a plasmon excitation, it is not possible with our experiment to distinguish between electron ejection via plasmon decay[3] or via plasmon-enhanced resonant electron-electron scattering, as was recently proposed.[17]

The effective solid angle of detection of the time-of-flight analyzer for slow ($\lesssim$10 eV) electrons was increased by applying a bias of +10 V to a grid at the entrance of the TOF

Published by the American Physical Society under the terms of the Creative Commons Attribution 3.0 License. Further distribution of this work must maintain attribution to the author(s) and the published article's title, journal citation, and DOI.

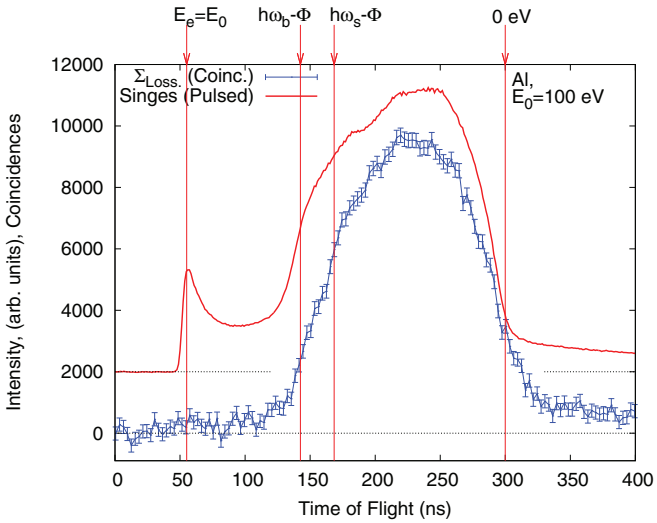

FIG. 1. (Color online) Time-of-flight (TOF) spectra for 100-eV electrons backscattered from polycrystalline Al. The (red) solid curve represents the singles spectrum. The (blue) data points represent the coincidence spectrum for primary electrons that have suffered an energy loss between 0 and 35 eV and correspond to the data in Fig. 2(b) integrated over the energy loss.

analyzer. This leads to flight times of slow electrons ($E \sim 0$ eV) of about 300 ns and, most importantly, to a significant increase of the coincidence count rates for small energies (~10 Hz with a ratio of true to false coincidences of $T/F \sim 0.2$ in Fig. 2 below). A pass energy of 50 eV was used in the HMA, leading to a resolution along the energy loss scale of 1.25 eV, and a resolution along the TOF scale (which is dominated by flight-time differences of trajectories with different radii in the HMA) of about 10 ns. The calculated energy-dependent transmission function of the TOF analyzer[15] was used to correct the double-differential spectra shown in Fig. 2.

The solid (black) curve in Fig. 2(a) is the experimental singles reflection-electron-energy-loss spectrum (REELS), and the (red) data points show the total number of coincidences as a function of the energy loss. The distribution of energy losses in individual bulk (differential inverse inelastic mean free path, DIIMFP) and surface losses (differential surface excitation probability, DSEP) are shown as curves peaking at the surface and bulk plasmon energy.[18] The theoretical curve for the DSEP exhibits a characteristic of the so-called "Begrenzungs" effect,[18,19] i.e., the complementarity between the surface and the volume plasmon, in that the DSEP exhibits a negative excursion exactly at the bulk plasmon frequency.

The coincidence spectra for energy losses of the scattered electron $\Delta E = E_0 - E_s$ between 0 and 35 eV (acquisition time 200 h) are shown in Figs. 2(b) and 2(c) and are compared with Monte Carlo simulations[18,20–22] in Fig. 3. The white parabolas in Figs. 2 and 3 represent energy conservation, i.e., flight times corresponding to ejected electrons escaping from the Fermi level with the full energy loss of the scattered electron minus the work function $E_e = \Delta E - \Phi$. The onset of coincidences is indeed observed exactly at $\Delta E = \Phi$ as a weak but very sharp ridge just below the energy-conservation line. The intensity of this ridge increases rapidly for larger losses, achieving its maximum around $\Delta E = \hbar\omega_s$ and abruptly decreasing at $\Delta E = \hbar\omega_b$. For energy losses just above the bulk plasmon energy, the coincidence count rate attains a minimum while it increases again for $\Delta E \gtrsim 2\hbar\omega_s = 21$ eV. For Al, this energy marks the boundary between the single- and the plural-scattering regime: As follows from the sharp single-scattering loss distributions in Fig. 2(a), energy losses below $2\hbar\omega_s$ can only take place in a *single* (surface or bulk) collision, while any larger energy loss involves plural inelastic scattering of the primary electron.

The Monte Carlo calculations follow the simulation model in Refs. 20 and 23 extended to account for a realistic depth dependence of the surface inelastic scattering cross section as described in Refs. 18,22, and 24 and appropriately accounts for surface excitations both inside the solid and in vacuum; the model was further extended to include secondary-electron emission following Refs. 4,21,22, and 25. The simulations are seen to agree reasonably with the experimental data. In order to obtain such agreement it is essential to take into account the following: (1) The depth dependence of the differential and integral surface excitation probability.[23] (2) SE generation at the very surface of the solid whenever a surface excitation takes place in vacuum.[26] (3) Creation of higher generation SEs. In the case of Al, this mainly concerns surface excitations suffered by first generation secondaries with energies of the order of $\hbar\omega_b$, which are very likely to suffer a surface energy loss since the surface excitation probability varies with kinetic energy as $E_k^{-1/2}$.[27] (4) The influence of electron refraction at the surface barrier (in the present work a value of $U_i = 15.4$ eV was used for the inner potential). The main shortcoming of the present simulations concerns the width of the surface plasmon features [see also Fig. 2(a)], which is due to the approximations made in the dielectric model.[18,23]

The fact that for $\Delta E \lesssim \hbar\omega_b$ the position and maximum of the ridge along the energy-conservation line coincide exactly with the surface plasmon features together with its abrupt decrease at $\Delta E = \hbar\omega_b$ allows one to conclude that this ridge is associated with a single surface excitation suffered by the backscattered electrons. From the narrow width of the ridge [see Fig. 2(c) in particular] it is concluded that the entire energy loss is transferred to a *single* ejected electron that escapes without noticeable further scattering.

At this stage it is important to recall that surface excitations take place in a very narrow depth range $\langle z_{ss} \rangle \sim \pm v/\omega_s$, a few angstroms on either side of the surface, where v is the electron speed.[26] In the case when the energy loss of the primary electron takes place in vacuum, i.e., a supersurface inelastic collision,[26] the question arises from what location is the SE emitted in such cases? In the simulations shown in Fig. 3 it is assumed that SE creation takes place at the very surface, $0 < z \ll 0.5$ Å. Most SEs then reach the detector without traversing the solid at all. Any other choice of the depth of origin leads to a strong reduction of the simulated intensity of the ridge below $\hbar\omega_b$, in clear contradiction with experiment. For subsurface energy losses, it is assumed that SE emission occurs at the location of the energy loss. The relative importance of super- and subsurface energy losses associated with penetration of the surface according to the model calculations is illustrated in Figs. 3(b) and 3(c), clearly showing the dominance of the supersurface scattering process.[26]

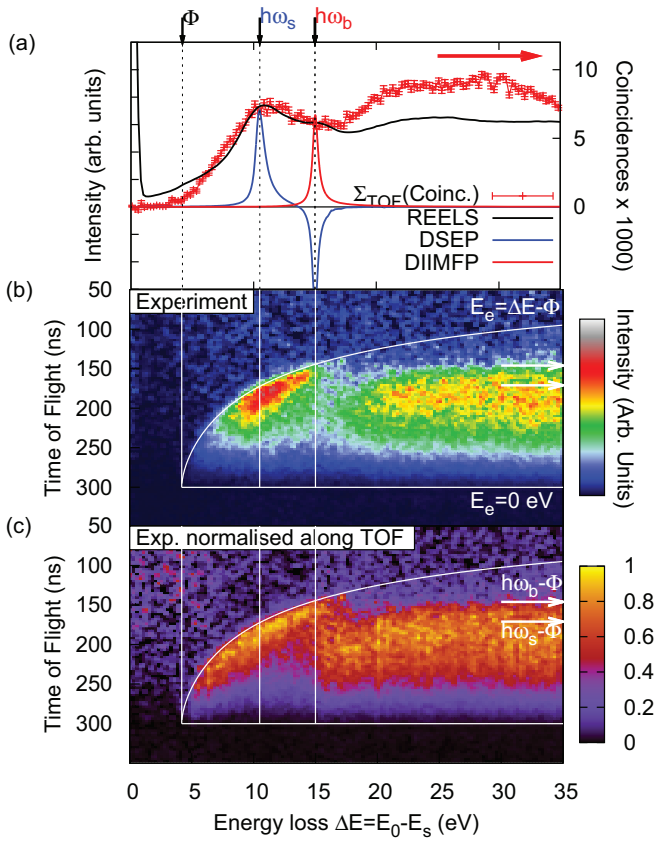

FIG. 2. (Color online) (a) Black solid curve: Experimental REELS spectrum. Thick (red) solid curve with datapoints (right axis): Integrated number of coincidences as a function of the energy loss. Blue and red solid curves: Bulk and surface single-scattering energy loss distribution (DIIMFP and DSEP). (b) Experimental SE2ELCS. (c) Same as (b) after normalizing the data for each energy loss to the intensity maximum along the time-of-flight scale.

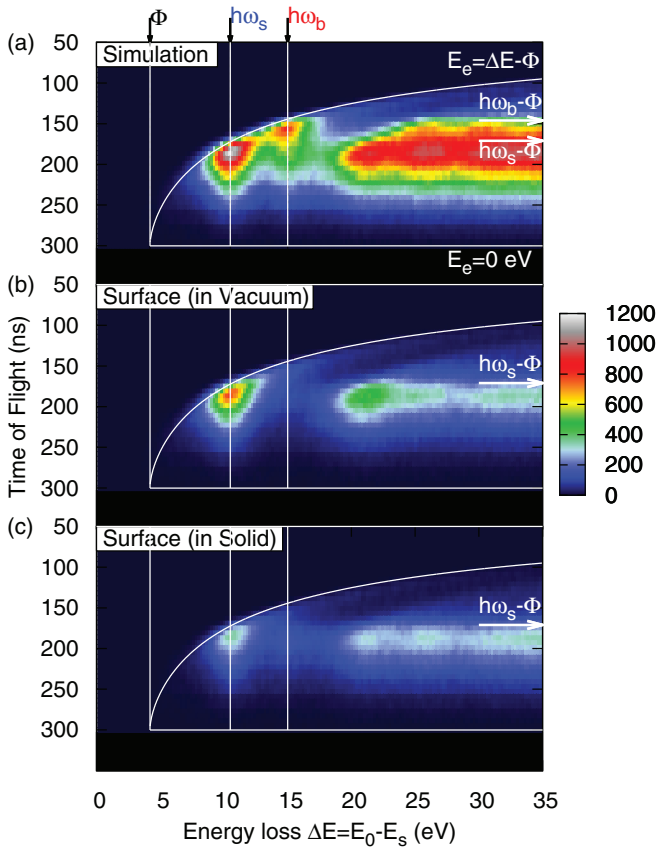

FIG. 3. (Color online) Results of Monte Carlo simulations for the coincidence spectra shown in Fig. 2(b). (a) Full simulation. (b) and (c) Contribution of surface excitations taking place in vacuum (b) and inside the solid (c).

The time-of-flight spectra of the ejected SEs change dramatically around and above $\Delta E \gtrsim \hbar\omega_b$, i.e., for energy losses for which the bulk loss mode sets in. Clearly, any difference between features seen at energy losses of, say, 14.5 and 15.5 eV cannot be attributed to the energy dependence of the electron-solid interaction characteristics, since all relevant physical quantities exhibit a smooth energy dependence. However, owing to the *Begrenzungs* effect and the resulting complementarity of surface and volume modes, the intensity of the volume modes in the surface scattering zone is strongly reduced by the very presence of the surface [cf. the negative excursion in the DSEP in Fig. 2(a)]. Therefore, processes with energy losses just above and below $\hbar\omega_b$ take place at markedly different depths. Furthermore, SEs created with energies of $\sim\hbar\omega_b$ are very likely to suffer energy losses before escape since the value of the inelastic mean free path (IMFP) is small for energies just above the bulk plasmon loss. The differential inelastic mean free path for such low energies does not resemble at all the sharply peaked curve shown in Fig. 2(a), which corresponds to 100-eV electrons, but is very broad. This explains the sudden decrease of intensity along the energy-conservation ridge and the broad structure in the coincidence time-of-flight spectra for $\hbar\omega_b \lesssim \Delta E \lesssim 2\hbar\omega_s$.

In the single-scattering regime, $\Delta E \lesssim 2\hbar\omega_s$, the number of coincidences in Fig. 2(a) is seen to follow the singles spectrum by a constant factor, while the plural-scattering regime above $\gtrsim 2\hbar\omega_s$ is clearly exposed in Fig. 2(a) by an increase in the number of coincidences relative to the singles signal. This is expected, since for Al any energy loss above $2\hbar\omega_s$ involves plural scattering.

Both in the coincidence SE spectrum and the singles spectrum in Fig. 1, features resulting from surface and volume plasmon decay[3,11,16] can be faintly discerned as shoulders appearing at $\hbar\omega_b - \Phi$ and $\hbar\omega_s - \Phi$. These features can also be identified (although less clearly) as a ridge at constant energy in Figs. 2 and 3 (see arrows). Note that this implies that individual energy losses of the primary electron are transferred to a *single* SE, since any physically realistic type of energy sharing in a three-electron process would lead to very broad spectra of the emitted SEs, lacking the characteristic energy loss of the surface and the bulk plasmon. Therefore, in the plural-scattering regime ($\Delta E \gtrsim 2\hbar\omega_s$) the SE spectrum consists of characteristic peaks at energies corresponding to surface and bulk plasmon decay, superimposed upon a broad and weak electron-electron scattering background extending up to the energy-conservation line.[11,16,28]

The similarity in the SE-coincidence and SE-singles spectra in Fig. 1 indicates that the above considerations also apply to the cascade regime for large energy losses $\Delta E \sim E_0$. While

this regime is characterized by multiple excitations of volume plasmons inside the solid, the corresponding SEs created upon plasmon decay have an energy less than 15 eV and therefore have a very large range inside the solid. However, when any of these SEs pass the surface scattering zone, they are very likely to participate in a surface energy loss after which their energy will (as a rule) be too low for them to overcome the surface barrier. The surface plasmon, however, will subsequently decay via emission of another secondary electron which has a high probability of escape and detection. This leads to a rather high contribution of surface energy losses to the SE yield for 100-eV primaries. According to the model calculations shown in Fig. 3 (that extend up to $\Delta E = E_0$, not shown) this contribution amounts to ∼40%. Furthermore, this contribution is only weakly dependent on the primary energy since the relative importance of surface losses as the final process in the cascade depends on the (characteristic) energy loss of the primary which is transferred to the cascade SEs rather than the energy of the primary electron.

Note that the validity of the above statements is by no means restricted to Al or the nearly free electron materials. While Al was chosen in the present work to expose the single- and plural-scattering regime and to clearly distinguish between surface and volume losses, many other materials[29] behave in exactly the same way in all relevant respects, although the (much broader) features in the electron-solid interaction characteristics would make identification of the supersurface secondary-electron emission process more complicated.

The processes described here should be of general relevance for SE emission near surfaces. This of course particularly concerns secondary-electron microscopy, for which the surface sensitivity is commonly interpreted merely in terms of the bulk stopping power of the solid. This leads to information depths of up to several tens of a nanometer. The present results emphasize that a realistic model for the surface sensitivity should take into account the influence of the surface leading to significantly smaller information depths. Furthermore, the observed supersurface secondary-electron emission process makes it possible to experimentally define the surface with unprecedented precision.

We thank P. Berlinger, R. Gärtner, and H. Schmidt for their expert assistance, which was decisive for the experimental work, and J. Kirschner, F. O. Schumann, J. Berakdar, N. Kouzakhov, and C. Lemell for stimulating discussions. Financial support by the Austrian Science Fund FWF (Project No. P20891-N20) is gratefully acknowledged. F.S-P. is thankful for a grant from the Fundación Caja Madrid and R.K. acknowledges support from a research scholarship of the Higher Education Commission of Pakistan.

*werner@iap.tuwien.ac.at

†Present address: Institut für Theoretische Physik, J. W. Goethe-Universität Frankfurt, Max-von-Laue-Strasse 1, 60438 Frankfurt/Main, Germany.

‡Present address: IMS Nanofabrication AG, Schreygasse 3, A-1020 Vienna, Austria.

[1] J. Goldstein, D. E. Newbury, P. Echlin, D. C. Joy, A. D. Romig, C. E. Lyman, C. Fiori, and E. Lifshin, *Scanning Electron Microscopy and X-ray Microanalysis* (Plenum, New York, 1992).

[2] C. V. von Koch, Phys. Rev. Lett. **25**, 792 (1970).

[3] M. S. Chung and T. E. Everhart, Phys. Rev. B **15**, 4699 (1977).

[4] J. P. Ganachaud and M. Cailler, Surf. Sci. **83**, 498 (1979).

[5] Y. Lin and D. C. Joy, Surf. Interface Anal. **37**, 895 (2005).

[6] D. Voreades, Surf. Sci. **60**, 325 (1976).

[7] F. J. Pijper and P. Kruit, Phys. Rev. B **44**, 9192 (1991).

[8] H. Müllejans and A. L. Bleloch, Phys. Rev. B **46**, 8597 (1992).

[9] J. Berakdar and J. Kirschner, *Correlation Spectroscopy of Surfaces, Thin Films, and Nanostructures* (Wiley-VCH, Weinheim, 2004).

[10] S. Samarin, J. Berakdar, A. Suvorova, O. Artamonov, D. Waterhouse, J. Kirschner, and J. Williams, Surf. Sci. **548**, 187 (2004).

[11] W. S. M. Werner, A. Ruocco, F. Offi, S. Iacobucci, W. Smekal, H. Winter, and G. Stefani, Phys. Rev. B **78**, 233403 (2008).

[12] B. D. Napitu and J. Berakdar, Phys. Rev. B **81**, 195108 (2010).

[13] F. O. Schumann, C. Winkler, and J. Kirschner, Phys. Rev. Lett. **98**, 257604 (2007).

[14] F. O. Schumann, C. Winkler, J. Kirschner, F. Giebels, H. Gollisch, and R. Feder, Phys. Rev. Lett. **104**, 087602 (2010).

[15] A. Bellissimo, R. Khalid, F. Salvat-Pujol, W. Smekal, and W. S. M. Werner, Rev. Sci. Instrum. (to be published).

[16] W. S. M. Werner, F. Salvat-Pujol, W. Smekal, R. Khalid, F. Aumayr, H. Störi, A. Ruocco, F. Offi, G. Stefani, and S. Iacobucci, Appl. Phys. Lett. **99**, 184102 (2011).

[17] K. A. Kouzakov and J. Berakdar, Phys. Rev. A **85**, 022901 (2012).

[18] F. Salvat-Pujol and W. S. M. Werner, Surf. Interface Anal. **45**, 873 (2013).

[19] R. H. Ritchie, Phys. Rev. **106**, 874 (1957).

[20] M. Novak, Surf. Sci. **602**, 1458 (2008).

[21] S. F. Mao, Y. G. Li, R. G. Zeng, and Z. J. Ding, J. Appl. Phys. **104**, 114907 (2008).

[22] F. Salvat-Pujol, Ph.D. thesis, Vienna University of Technology, 2012.

[23] Y. C. Li, Y. H. Tu, C. M. Kwei, and C. J. Tung, Surf. Sci. **589**, 67 (2005).

[24] Z.-J. Ding, H. M. Li, Q. R. Pu, Z. M. Zhang, and R. Shimizu, Phys. Rev. B **66**, 085411 (2002).

[25] A. Dubus, J.-C. Dehaes, J.-P. Ganachaud, A. Hafni, and M. Cailler, Phys. Rev. B **47**, 11056 (1993).

[26] W. S. M. Werner, M. Novak, F. Salvat-Pujol, J. Zemek, and P. Jiricek, Phys. Rev. Lett. **110**, 086110 (2013).

[27] W. S. M. Werner, Surf. Sci. **604**, 290 (2010).

[28] This $(e,2e)$ background (Ref. 16) is strongly suppressed in the present data due to the energy dependence of the transmission function when the TOF spectrometer is biased (Ref. 15).

[29] W. S. M. Werner, C. Ambrosch-Draxl, and K. Glantschnig, J. Phys. Chem. Ref. Data **38**, 1013 (2009).